Ultra-fast fMRI imaging with high-fidelity activation map

Neelam Sinha[1], Manojkumar Saranathan[1], A. G. Ramakrishnan[1], Juan Zhou[2], and Jagath C. Rajapakse[2]

[1] Indian Institute of Science, Bangalore, India
{neelam,manojk,ramkiag}@ee.iisc.ernet.in
[2] NTU, Singapore
{zhou0025,asjagath}@ntu.edu.sg

Abstract. Functional Magnetic Resonance Imaging (fMRI) requires ultra-fast imaging in order to capture the on-going spatio-temporal dynamics of the cognitive task. We make use of correlations in both k-space and time, and thereby reconstruct the time series by acquiring only a fraction of the data, using an improved form of the well-known dynamic imaging technique k-t BLAST (Broad-use Linear Acquisition Speed-up Technique). k-t BLAST (k-tB) works by unwrapping the aliased Fourier conjugate space of k-t (y-f space). The unwrapping process makes use of an estimate of the true y-f space, obtained by acquiring a blurred unaliased version. In this paper, we propose two changes to the existing algorithm. Firstly, we improve the map estimate using generalized series reconstruction. The second change is to incorporate phase constraints from the training map. The proposed technique is compared with existing k-tB on visual stimulation fMRI data obtained on 5 volunteers. Results show that the proposed changes lead to gain in temporal resolution by as much as a factor of 6. Performance evaluation is carried out by comparing activation maps obtained using reconstructed images, against that obtained from the true images. We observe upto 10dB improvement in PSNR of activation maps. Besides, RMSE reduction on fMRI images, of about 10% averaged over the entire time series, with a peak improvement of 35% compared to the existing k-tB, averaged over 5 data sets, is also observed.

1 Introduction

Magnetic resonance imaging (MRI) has emerged as a powerful tool in medical imaging and diagnosis in the last decade, due to its non-invasive nature and excellent soft-tissue contrast. Although high spatial resolution images are essential in medical diagnosis and image analysis, high temporal resolution is critical in applications like dynamic contrast-enhanced MRI or functional MRI (fMRI), where dynamic events are monitored. Today, fMRI has the potential to probe neurophysiological activation in the brain at a much higher spatial resolution than that offered by other non-invasive neuroimaging techniques like PET. The

high sensitivity measurement of blood oxygenation level dependent (BOLD) signal modulation points to regions in the cortex responsible for the underlying activity. Currently fMRI applications interrogate neural activity changes only on the order of seconds, although neural activity happens on time scales of the order of milliseconds. One way of increasing the temporal resolution is to reconstruct high quality images from partial data. Parallel imaging methods can also be used to achieve accelerated imaging, but they require customized hardware. Parallel imaging involves utilizing an array of receiver coils with varying coil sensitivities, instead of a single coil, with homogeneous sensitivity.

In MRI, data is sampled in the spatial frequency domain of the object being imaged (called k space), directly leading to the well known trade-off between temporal and spatial resolution. Parallel imaging techniques [1, 2] are gaining popularity but they require customized hardware. However, partial data-based reconstruction have no such requirements. Partial data acquisition involves acquiring a pre-determined region in k-space. Many techniques like Keyhole [3], Reduced encoding Imaging by Generalized series Reconstruction (RIGR) [4], Two-reference Reduced encoding Imaging by Generalized series Reconstruction (TRIGR) [5], Unaliasing by Fourier-Encoding the Overlaps Using the Temporal Dimension (UNFOLD) [6], k-t BLAST [7], that reconstruct images from partial data, have been reported. Some of the methods use direct replacement, while others extrapolate the missing values using correlations in k-space and/or time. Keyhole is the simplest known technique where during the course of dynamic changes only low frequencies in k-space are acquired, while the unacquired high frequencies are simply replaced by the corresponding values obtained from a static high-resolution acquisition. However, discontinuities in reconstructed k-space lead to artifacts in images, and hence higher acceleration factors cannot be explored. Methods like RIGR and TRIGR use generalized-series modeling to estimate the unacquired values in k-space. High resolution static images serve as estimates to obtain the corresponding values at instants of dynamic changes. Both these methods linearly fit the unacquired values in terms of the acquired data, and basically solve a system of linear equations. Reported works using these methods claim acceleration factors of 4-6. However, methods like UNFOLD and k-tB are radically different from the above. They employ a sparse acquisition scheme that results in a known form of aliasing that is eventually unwrapped either using temporal filtering (UNFOLD) or using a low resolution, alias-free training map (k-tB). In this paper, we propose changes to two aspects of the existing k-tB algorithm. Firstly, the estimates obtained from the training map are improved using generalized series modeling (labelled as RIGR in further references). The second proposed change is the incorporation of phase constraints obtained from the alias-free training map. These two changes together were utilized for reconstruction of fMRI data sets obtained from a photic stimulation experiment, and improvements in resulting images were quantified. The overview of the proposed method is shown in Fig. 1. The paper is organised as follows. The theory of k-tB is given in section 2, followed by the variations proposed

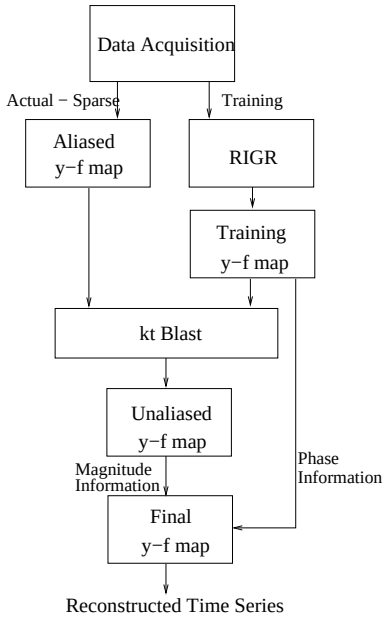

Fig. 1. Overview of the proposed method

to the existing technique in section 3. The data used and results obtained are discussed in section 4. Finally, section 5 concludes the paper.

2 *k-t* BLAST

k-t BLAST, was proposed by Tsao et. al [7], for reconstruction of dynamic images using sparsely acquired data. The correlations in both *k*-space and time are exploited for estimating the unacquired data. A missing data point is estimated based on other available points, within its vicinity in both *k*-space and time. The advantage of this approach is that it exploits more of the relevant correlations, thus improving the estimation of missing data. This improvement could be used to obtain better reconstructed images error or achieve higher reduction in data acquisition leading to better temporal resolution.

Dynamic MRI can be seen as acquisition of a changing *k*-space signal at different time instants, which is essentially sampling in a higher dimensional *k-t* space. Here, *k* stands for multi-dimensional *k*-space. Since we are dealing with $2D$ *k*-space, and it is known that all points along the read-out (k_x) dimension are available, we need to undersample only along phase-encode dimension (k_y). Hence, the mention of *k*-axis would refer to the actual k_y axis, whose Fourier conjugate axis would be the spatial dimension y. The lattice along which these points are acquired in *k-t* space is referred to as the *k-t* sampling pattern. The conjugate space obtained upon Fourier transformation of the *k-t* space is the

y-f space. It is observed that the signal distribution in y-f space is very sparse, especially for fMRI with its temporal periodicity of activated pixels. This feature can be used to pack y-f space densely allowing higher acceleration factors. Under-sampling in k-t space leads to an aliased signal distribution in y-f space. For instance, at a given location (y_0, f_0) in the aliased y-f space obtained from the sparsely acquired data, the signal value $\rho_{alias}(y_0, f_0)$ is actually the sum of the values at $(y_1, f_1) \ldots (y_n, f_n)$ on the true y-f space signal distribution. The locations $(y_1, f_1) \ldots (y_n, f_n)$ in (1) are determined by the k-t sampling pattern.

$$\rho_{alias}(y_0, f_0) = \rho_1(y_1, f_1) + \ldots + \rho_n(y_n, f_n) \tag{1}$$

where, n is acceleration factor.

Unaliasing the aliased y-f signal distribution becomes possible because the aliasing pattern is completely known once the sampling pattern is fixed. This set of under-determined system of equations given by (1) needs to be solved for every set of aliased voxels. Since, infinite solutions exist, the most sensible way would be to minimize a well-designed cost function. Here, weighted-minimum norm solution is preferred. This solution makes use of prior information, wherein a low resolution, alias-free signal distribution is obtained by acquiring the low k-space frequencies, forming the "training map". The values of the training map form initial estimates in order to obtain the solution as given in (2). Note that the acquisition of the training map data slightly reduces the speed-up effected by the under-sampling pattern.

$$\rho = \mathbf{M}^2.\mathbf{1}^H(\mathbf{1}.\mathbf{M}^2.\mathbf{1}^H)^{-1}.\rho_{alias} \tag{2}$$

where, $\mathbf{M}^2 = diag(|m_1|^2, \ldots |m_n|^2)$, and $|m_i|$ is the magnitude of the training y-f map at the ith aliasing location. Here, $\mathbf{1}$ is the row vector of all 1s, at n positions. The DC-value however, is separately taken care of, since it is the most important component. The temporal average of the sparse acquisitions forms the DC-value of the estimated y-f map.

The new set of equations to be solved is now as in (3).

$$\rho = \underline{\rho} + \mathbf{M}^2.\mathbf{1}^H(\mathbf{1}.\mathbf{M}^2.\mathbf{1}^H + \psi)^{-1}.(\rho_{alias} - \mathbf{1}\underline{\rho}) \tag{3}$$

where, $\underline{\rho}$ is the baseline estimate (DC-component) and ψ is the noise variance.

3 Proposed Method

3.1 Data acquisition schemes

In the original k-tB scheme [7], the training and actual data acquisitions are done at disjoint instants of time, and follow different sampling schemes [8]. The training data samples only low-frequency k-space data, while the actual data acquisition is along a pre-designed sparsely sampled lattice, as shown in Fig. 2(a). A variation of data acquisition scheme that couples both the training and actual scans is shown in Fig. 2(b). This is a variable density sampling lattice.

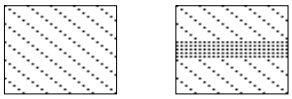

(a) (b)

Fig. 2. Data acquisition (a) Uniform density (Existing) (b)Variable density (Utilized)

This scheme was chosen in order to minimize the mismatch between training and data scans. This scheme of acquisition reduces the acceleration factor achievable, but eliminates possible artifacts due to mis-registration. In our trials, we utilized this variable-density sampling scheme.

3.2 Training map

The reported work of Hansen et al [9], deals with how the quality of training data influences the working of k-tB, in contexts where training and actual data are acquired at disjoint instants of time. It reports that increasing the number of time frames for which the training data is acquired, results in only a negligible decrease of reconstruction error. It also reports that filtering of the training data in order to reduce truncation artifacts had minor impact on reconstruction errors. However, in a variable-density acquisition scheme like ours, training data is available at all time frames of the experiment. We explored the impact of including higher frequencies in the training data, on the working of k-tB. We compared k-tB reconstructions that use low resolution training data against k-tB reconstructions that use all the frequencies (ideal training) in the training map. It is seen that the errors can be brought down using higher frequencies in the training map, by a factor of 2. The disparity in the two reconstructions led us to explore the possibility of obtaining an improved resolution training-map using the acquired low frequencies. It must be observed that at locations in the aliased y-f space, where the signal is dominated by noise, the values from the training map that are chosen as estimates, can lead to meaningful results only if the estimate is close to the truth.

3.3 Proposed variations to k-tB

The proposed method generates an improved-resolution training map, despite acquiring only the lower spatial frequencies. This is done by extrapolation using the generalized series model, which requires one full-resolution acquisition. The high-resolution static acquisition serves to estimate the missing high-frequencies in the training map. The working of the generalized series modeling is outlined below.

Generalized series modeling : In generalized series modeling, the missing high spatial frequencies is split into two components as shown in (4). The first

part comes from the *apriori* static information, whereas the second part comes by adaptively adjusting the coefficients so that data consistency is maintained.

$$d_{GS}(k) = d_c(k) + \sum_m c_m d_c(k - m.\Delta k) \tag{4}$$

where, d_{GS} is the Generalized series estimate, d_c is the Fourier transform of the static image, c_m are the generalized series coefficients and Δk refers to the spatial-frequency resolution. A fast version of this algorithm outlined in [5] is used for implementation. After this extrapolation, it follows that the deviation of the training data from the ideal, full k-space training data decreases. We expect better training data to translate to better training maps in y-f space.

Phase constraints : The second change proposed is the incorporation of phase constraints from the training map. The training map, though not of best possible resolution, however does contain unaliased signal distributions. In (3), as given in the original k-t BLAST proposition, the phase of the aliased y-f map is used, which would be erroneous. Hence, we use the phase information of the training map in estimating the true y-f map.

$$\Theta = \angle \rho_{train} \tag{5}$$

$$\tilde{\rho} = |\rho| \exp(i\Theta) \tag{6}$$

where, $\tilde{\rho}$ is the final estimate of the signal distribution in y-f plane. ρ_{train} is the training map.

4 Results and Discussion

4.1 Data description

fMRI data was obtained for experiments with "visual stimulus" While a subject performed the experiment, 3 two-dimensional T*2-weighted images, each with 64 scans, were acquired using a gradient-echo FLASH sequence (TE/TR 40msec/80.5msec, matrix = 128 × 64; The image matrices were zero-filled to obtain 128 × 128 images with a spatial resolution of 1.953 × 1.953 mm; slice thickness = 5-mm and 2-mm gap). The corresponding two-dimensional anatomical slices were also acquired with a T1-weighted IR RARE sequence (TI = 900 msec; TE/TR 3900msec/40msec, matrix = 512 × 512) in the same experiment session. In all experiments, ON and OFF stimuli were presented at a rate of 5.162 sec/sample. Each stimulation period had four successive stimulation ON states followed by four stimulation OFF states. The stimulations were repeated for eight cycles (total experiment time = 5.5 min), and experiments were carried out at different sessions with different subjects. The visual stimulation task comprised an 8-Hz alternating checkerboard pattern with a central fixation point projected on a LCD system. The subjects were asked to fixate on the point during stimulations. Images were acquired at three axial levels of the brain at the visual cortex.

4.2 Performance evaluation

fMRI images are mainly studied for the activation maps which interpret the information contained in the entire time series of images. Hence, to evaluate the reconstruction performance, we compare the activation maps obtained against the reference activation map. Statistical Parametric Mapping (SPM) is the most widely used method for fMRI time-series analysis [10]. The software package SPM2, that implements SPM, downloaded from [11], was used for analysis. The primary objective is to detect activated voxels and the resulting statistical parametric maps represent the activation strength of each voxel. The scale of the activation-strength obtained is important, since the activation maps are eventually thresholded to obtain truly activated regions. Hence when drastic changes in the scales of activation-strength are observed, the activation maps are considered degraded. Root Mean square error (RMSE), correlation with reference, and mean activation level of the activation maps are used to quantify the degradation in activation. If we analyze the true image time series A and the reconstructed series B, using same SPM method and parameters, we expect comparable scales in activation strength at similar locations, in the resulting statistical parametric maps S_A and S_B. fMRI time-series are first realigned to remove movement effects using least-squares minimization [10] and then smoothed with Full Width at Half Maximum (FWHM) = 4.47mm, 3D Gaussian kernel to decrease spatial noise. Canonical hemodynamic response function (HRF) plus time and dispersion derivatives is used as basis function and changes in BOLD signal associated with the task were assessed on a pixel-by-pixel basis, using the general linear model and the theory of Gaussian fields as implemented in SPM2. This method takes advantage of multivariate regression analysis and corrects for temporal and spatial autocorrelations in the fMRI data. Voxels in the statistical parametric map based on F-contrast below a threshold of $p \leq 0.05$ are identified as activation, which was corrected for multiple comparisons using family-wise-error (FWE).

4.3 Experimental results

MATLAB was used for all simulations. For our trials, the training and actual acquisitions were generated from the full resolution true k-space, by using the appropriate sub-sampling masks. The images of training as well as sparse y-f maps are shown in Fig.3(a and b, respectively). As claimed earlier, it can be seen that the signal distribution in y-f space is very compact, thus leading to possibilities of achieving higher acceleration factors. In Fig.4 (a), the deviation of the training data with respect to the ideal data is shown in 2 cases. In the first case, the training data is simply zero-padded as in the existing (baseline) k-tB, where as in the second case, the obtained low frequencies are RIGR-extrapolated (proposed). Clearly, the RIGR-extrapolated data is seen to be closer to the truth. In Fig.4 (b), we compare how the gains of Fig.4 (a), translate in the y-f space. It can be observed that the RIGR-extrapolated training map is close to the training map that would have been generated had all the frequencies been available for

(a) (b)

Fig. 3. Typical y-f maps obtained for acceleration factor 5 using (a) Training data (b) Actual data

training (ideal/full training) and is more accurate than the zero-padded map that the original k-tB algorithm uses. In Fig. 5 (a), we see errors in the reconstructed

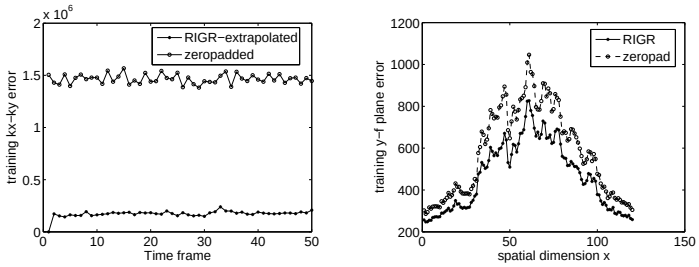

(a) (b)

Fig. 4. Errors for acceleration factor 5 in (a) Training k-space data (b) y-f-Training map

y-f plane as compared to the true y-f plane. The three cases compared are : The training map being ideal (full training), zero-padded (baseline k-tB) and RIGR-extrapolated (proposed). It can be seen that the RIGR-extrapolated case results in lower errors compared to the zero-padded case, consistently for all instants of the time series. In Fig. 5 (b) the time series of errors in RMSE, incurred during image reconstruction in all the three cases outlined above, is shown. It can be seen that the RIGR-extrapolated case and the ideal training map case, are quite comparable, while both consistently outperform the baseline k-tB reconstruction. Fig. 5(c) shows the decline in correlation of the obtained activation map with the reference map, against acceleration factor.

In Fig.6, we observe the activation maps obtained using the two methods, for a gain of factor 5 in temporal resolution. Clearly, the map obtained using Baseline k-tB displays more artifacts than the proposed method. We also observe that the gain in PSNR goes upto 10dB. The RMSE of the fMRI time series reduces

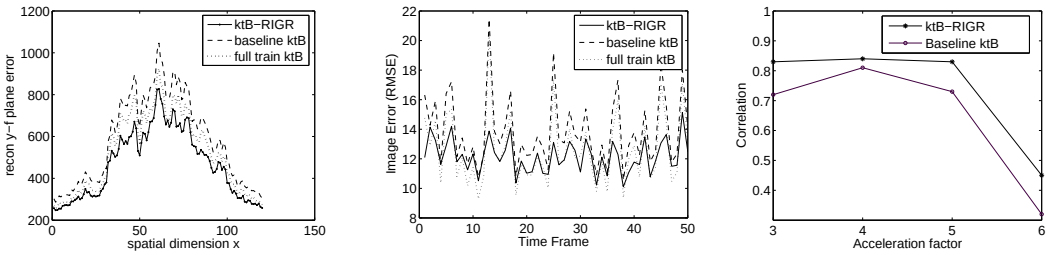

(a) (b) (c)

Fig. 5. Reconstruction errors for acceleration factor 5 in (a) y-f map (b) Image series (RMSE) ; (c) Correlation with reference activation map

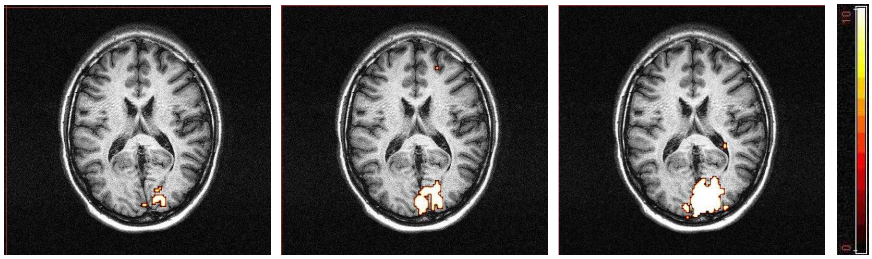

(a) (b) (c)

Fig. 6. Thresholded Activation maps obtained using SPM for acceleration factor 5 (a) True Images (b) Proposed method (c) Baseline ktB

by about 10% averaged over all time points, with a peak improvement of 35% compared to the existing k-tB for acceleration factors upto 6. For acceleration factor of 6 we notice that the scales of activation maps obtained using baseline k-tB are lower by a factor more than 10, and hence it is not possible to threshold them to see activated regions. On the other hand, the proposed method results in activation maps that are lower by a factor 2 and hence activated regions can be seen at lower thresholds. At accelerations above 6 we notice significant degradation in the strength scales of the activation maps, and hence do not consider them.

We also carried out trials where only one of the two proposed changes were made to the existing algorithm. We first chose to extrapolate training data and skip the incorporation of phase constraints. It was observed that the resulting reconstructions did not show much change when compared against the case where zero-padded training data was used. In this case, we know that the best possible reconstruction achievable is what results out of using the ideal training set. In the next trial, we retained the zero-padded training map, and incorporated only the phase constraint. It was seen that this worsens the performance of the baseline k-tB, since the phase map imposed is a blurred version of the original. Hence, it is

observed that incorporating both changes leads better reconstruction compared to the baseline k-tB.

5 Conclusion

In this paper, we have proposed an improved version of the existing dynamic imaging technique k-tB. The changes include improvement in the training map that serves as an estimate to obtain the true signal distribution. The other proposed change is the utilization of the phase-constraints from the training map, rather than the aliased map. Trials on real fMRI data have shown that these 2 changes together lead to improved reconstructions and acceleration factors of upto 6. The reconstruction performance is evaluated using activation maps obtained. We observe upto 10dB improvement in PSNR of activation maps. The proposed technique results in more accurate activation maps and also the image time series incurs mean RMSE of less than 10% averaged over the entire time series, for acceleration factors upto 6.

References

1. Pruessmann, K.P., Weiger, M., Scheidegger, M.B., Boesiger, P.: Sense : Sensitivity encoding for fast mri. Magnetic Resonance in Medicine **42** (1999) 952–962
2. Sodickson, D.K., Manning, W.J.: Simultaneous acquisition of spatial harmonics (smash): ultra-fast imaging with radio frequency coil arrays. Magnetic Resonance in Medicine **38** (1997) 591–603
3. van Vaals, J.J.: Keyhole method for accelerating imaging of contrast uptake. Journal of Magnetic Resonance Imaging **3** (1993) 671–675
4. Liang, Z.P., Lauterbur, P.C.: An efficient method for dynamic magnetic resonance imaging. IEEE Transactions on Medical Imaging **13** (1994) 677–686
5. Liang, Z.P., Madore, B., Glover, G.H., Pelc, N.J.: Fast algorithms for gs-model-based image reconstruction in data-sharing fourier imaging. IEEE Transactions on Medical Imaging **22** (2003) 1026–1030
6. Madore, B., Glover, G.H., Pelc, N.J.: Unaliasing by fourier-encoding the overlaps using the temporal dimension (unfold), applied to cardiac imaging and fmri. Magnetic Resonance in Medicine **42** (1999) 813–828
7. Tsao, J., Boesiger, P., Pruessmann, K.P.: k-t blast and k-t sense: Dynamic mri with high frame rate exploiting spatiotemporal correlations. Magnetic Resonance in Medicine **50** (2003) 1031–1042
8. Tsai, C.M., Nishimura, D.G.: Reduced aliasing artifacts using variable-density k-space sampling trajectories. Magnetic Resonance in Medicine **43** (2000) 452–458
9. Hansen, M.S., Kozerk, S., Pruessmann, K.P., Boesiger, P., Pedersen, E.M., Tsao, J.: On the influence of training data quality in k-t blast reconstruction. Magnetic Resonance in Medicine **52** (2004) 1175–1183
10. Friston, K.J., Holmes, A.P.: Statistical parametric maps in functional imaging: A general linear approach. Human Brain Mapping **2** (1995) 189–210
11. http://www.fil.ion.ucl.ac.uk/spm/software/spm2/.